SCIENTIFIC PAPERS
OF THE UNIVERSITY OF PARDUBICE
Series B
The Jan Perner Transport Faculty
11 (2005)

DYNAMICS OF A TWO - PHASE FLUID ALTERNATING FLOW (FAF) MECHANISM WITH A LINEAR HYDRAULIC MOTOR

Jozef TURZA [1], Monika GULLEROVÁ [2]

[1] Faculty of special Technologies, Alexander Dubcek University in Trencin, SR
[2] Institut of Natural and Humanit Sciences, Alexander Dubcek University in Trencin, SR

PROLOGUE

Besides conventional parallel flow hydraulic sets, units with alternating fluid flow proved their significance in the practice. As for parallel flow sets, the fluid flows in the line between the hydraulic pump and the hydraulic motor in one direction. However, the fluid in mechanisms with alternating flow in the line makes a reverse motion. When stabilized both flow and pressure are periodical. In spite of the fact that there are several kinds of mechanisms with the fluid alternating flow (FAF) as for the number of phases (lines), extensive application of double-phase units with FAF is expected. The can be applied in any equipment that requires constant alternating motion of the element (hydraulic motor), e.g. agricultural mowers, machine shaking junctions, looms for textile industry, equipment for fatigue tests, etc. When comparing them with conventional cam or crank units, their principal advantages rest with independent spatial arrangement on machines and simple overload protection.

Dynamic analysis is critical to evaluate functional and dynamic properties of a two-phase mechanism. Let us make a model analysis of the double-phase mechanism with FAF consisting of a rotary hydraulic pump and linear hydraulic motor.

1. INTRODUCTION

We will analyze internal behavior of the double-phase hydraulic mechanism with FAF consisting of a rotary hydraulic pump *HG* and a linear hydraulic motor *HM* as shown in *Fig. 1*. We shall apply the method used in mechatronics [7] which takes into account the interaction of an element with its respective environment through power transfer.

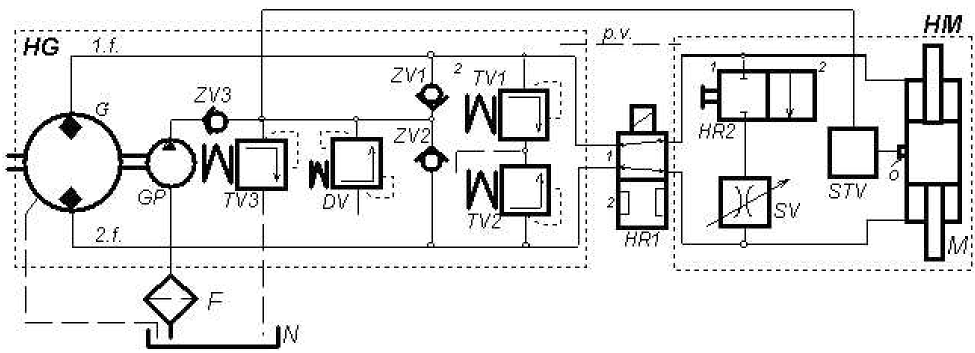

Fig. 1 Diagram of the double-phase mechanism with FAF fitted with a linear hydraulic motor

Phases of the hydraulic pump *HG* and the hydraulic pump *HM* are designated as *1.f.* and *2.f.* as shown in *Fig. 1*. They are interconnected by a four-way double-position distributor *HR1*. Its function is to connect and disconnect the hydraulic motor. Hydraulic pump *HG* phases are fitted with pressure valves *TV1* and *TV2* which serve as overload protection. Hydraulic pump *HG* is equipped with auxiliary unidirectional hydraulic pump *PG*. It is there to replenish flow leakages, to provide the hydraulic circuit with protection against pressure drop in phases below the value representing the saturated steams pressure of the fluid used in the circuit and with circuit rinsing. The auxiliary hydraulic circuit has a built-in pressure valve *TV3* and check valve *ZV3.*

The phases of the main circuit are replenished in an alternating way by means of the auxiliary hydraulic pump circuit check valves *ZV1* and *ZV2.* Phases of the hydraulic motor *HM* are also interconnected with a two-way double position distributor *HR2* and a throttle valve *SV*. When changing the distributor *HR2* to its No. *2* position and setting the throttle valve *SV*, it is possible to control smoothly the stroke amplitude of the linear hydraulic motor *M*.

It is possible to stabilize a central position of the hydraulic motor *M* by means of stabilization pressure valve *STV* and its control edges *o*. Filter *F* is used to filter the hydraulic circuit fluid.

2. EQUIVALENT STRUCTURE OF THE CIRCUIT

In order to make a circuit internal analysis covered in *Fig. 2*, circuit equivalent structure will be employed. Consequently, DYNAST software will be applied to make the analysis. Equivalent structure is shown in *Fig. 2*.

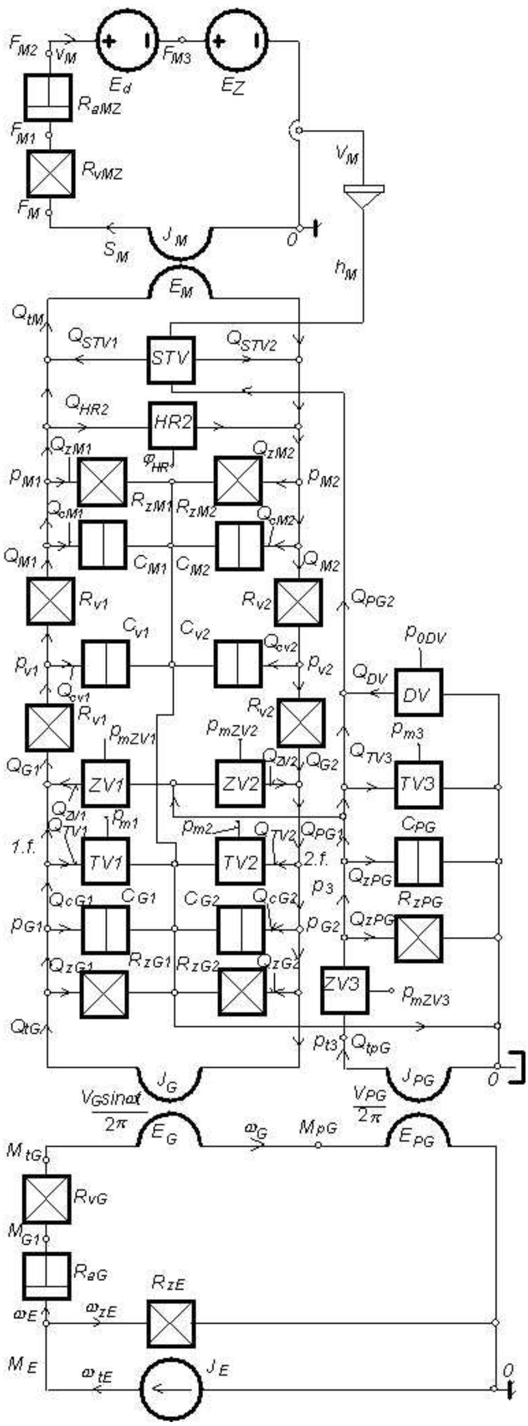

Fig. 2 Circuit equivalent structure inside double-phase mechanism with FAF fitted with linear hydraulic motor

The structure does not include the hydraulic distributor *HR1.* Fixed source of rational speed marked J_E was selected to make the position stabilization effect clearer.

The equivalent structure as shown in *Fig. 2* complies with types of a power carrier and notions as usual in respective engineering fields. The left hand part covers the source of rational speed, voltage quantity is represented by torque and current quantity by angular velocity (M, ω). In the central part, fluid serves as power carrier, voltage quantity is represented by pressure and current quantity by flow (Q, p). The right hand part shows a solid carrier making linear motion, having voltage quantity represented by force, current quantity by hydraulic motor motion speed (F, v).

A transformer is used to separate the aforementioned parts. In the first case, the transformer is replaced by the moment source E_G and fluid flow source J_G. In the second case, the transformer is replaced by pressure source E_M and speed source J_M. Moment E_{PG} and flow J_{PG} sources are both used to replace the auxiliary hydraulic pump *PG* transformer. Markings R_{zG1}, R_{zG2} stand for hydraulic pump *G* leakage flows, C_{G1}, C_{G2} denote hydraulic pump *G* and hydraulic motor *M* phase capacities. Next, sources J_{ZV1}, J_{ZV2} denote pressure control valve properties *VT1* and *VT2.* In addition, sources J_{ZV1}, J_{ZV2} denote check valve properties *ZV1* and *ZV2* fed from a line of the auxiliary hydraulic pump *PG*.

Source J_{stM} represents a position stabilization system of the hydraulic motor *M*, R_{zpG} denotes leakage resistance of auxiliary hydraulic pump *PG*, C_{PG} denotes line capacity of the auxiliary hydraulic pump *PG*, source J_{TV3} marks pressure control valve properties of the auxiliary hydraulic pump circuit *PG*, R_{vMZ} denotes a viscous friction coefficient (inner resistance) of the hydraulic motor *M* and the load. E_d stands for the force source providing characteristics of hydraulic motor stops in its end position, E_Z denotes constant force from the load (irrespective of the hydraulic motor speed) and finally R_{aMZ} denotes the mass of hydraulic motor and load.

3. CIRCUIT ANALYSIS

Analysis was made in line with specifications as provided in Figure 2 using the DY-NAST software. Specifications were used as follows: geometric displacement volume of hydraulic pump and hydraulic motor of $V_G = V_M = 25\ \mathrm{cm}^3$, phase line length of $L = 4$ m, load mass of $m = 0.5$; 4; 8 kg, viscous damping coefficient of $R_{vMZ} = 0.1$; 10 and 20 $\mathrm{N \cdot m^{-1} \cdot s}$ and source speed of $n = 10$ and 25 $\mathrm{s^{-1}}$ from the starting phase up to stabilization of periodical course of both pressure and flow. Basic parameters being changed are provided in figures to follow.

Following equations will be used for double phase mechanisms as shown in *Fig. 2*. Electric motor *E* as shown in *Fig. 3*.

$$\omega_E = 2\pi \cdot n_E \cdot f_E(t) - \frac{M_E}{R_{zE}}, \quad \omega_G = \omega_E \tag{1}$$

$$f_E(t) = \frac{t}{t_1}, \text{ for } 0 \le t < t_1, \tag{2}$$

$$f_E(t) = 1 \text{ for } t > t_1, \tag{3}$$

$$M_E = M_G. \tag{4}$$

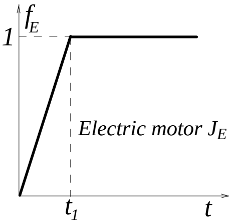

Fig. 3 Behavior of the function f_E

Hydraulic pump *G*:

$$M_G = M_{tG} + M_{pG} + R_{aG} \cdot \frac{\dot{\omega}}{2\pi} + R_{vG} \cdot \frac{\omega_E}{2\pi}, \text{ moment of the pump} \tag{5}$$

$$M_{tG} = (p_1 - p_2) \cdot \frac{V_G}{2\pi} \cdot \sin(\omega_E \cdot t) / \eta_{mG}, \text{ theoretical moment of the pump G} \tag{6}$$

$$Q_{G1} = Q_{tG} - Q_{zG1} - Q_{cG1} - Q_{TV1} + Q_{ZV1}, \text{ hydraulic pump flow 1.f.} \tag{7}$$

$$Q_{G2} = Q_{tG} + Q_{zG2} + Q_{cG2} + Q_{TV2} - Q_{ZV2}, \text{ hydraulic pump flow 2.f.} \tag{8}$$

$$Q_{Gt} = V_G \cdot \frac{\omega_G}{2\pi} \cdot \sin(\omega_E \cdot t) / \eta_{mG}, \text{ theoretical hydraulic pump flow G} \tag{9}$$

$$Q_{zG1} = \frac{1}{R_{zG1}} \cdot p_{G1}, \text{ hydraulic pump flow leakage 1.f.} \tag{10}$$

$$Q_{zG2} = \frac{1}{R_{zG2}} \cdot p_{G2}, \text{ hydraulic pump flow leakage 2.f.} \tag{11}$$

Pressure control valve *TV1* flow 1.f.

as shown in *Fig. 4*:

$$Q_{TV1} = \frac{p_{G1} - p_{m1}}{R_{TV1}}, \text{ for } (p_{G1}-p_{m1})>0, \tag{12}$$

$$Q_{TV1} = 0, \text{ for} (p_{G1}-p_{m1}) \le 0, \tag{13}$$

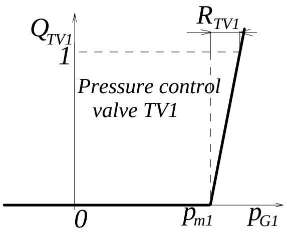

Fig. 4 Behavior of pressure control valve flow TV1

Pressure control valve *TV2* flow 2.f.

as shown in Fig.5:

$$Q_{TV2} = \frac{p_{G2} - p_{m2}}{R_{TV2}}, \quad \text{for } (p_{G2}\text{-}p_{m2}) > 0, \qquad (14)$$

$$Q_{TV2} = 0, \quad \text{for } (p_{G2}\text{-}p_{m2}) \le 0, \qquad (15)$$

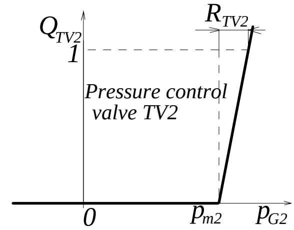

Fig. 5 Behavior of pressure control valve flow TV2

Pressure control valve *TV3* PG as shown in Fig. 6:

$$Q_{TV3} = \frac{p_3 - p_{m3}}{R_{TV3}}, \quad \text{for (p3-pm3)} > 0, \qquad (16)$$

$$Q_{TV3} = 0, \quad \text{for (p3-pm3)} \le 0. \qquad (17)$$

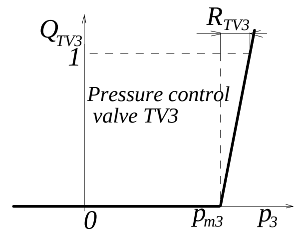

Fig. 6 Behavior of pressure control valve flow TV2

Capacity flow *G* 1.f. a 2.f.:

$Q_{cG1} = C_{G1} \cdot \dot{p}_{G1}$, pump capacity flow *G* 1.f. (18)

$Q_{cG2} = C_{G2} \cdot \dot{p}_{G2}$, pump capacity flow *G* 1.f. (19)

$C_{G1} = \dfrac{V_{v1}}{K_k}$, capacity 1.f. (20)

$C_{G2} = \dfrac{V_{v2}}{K_k}$, capacity 2.f. (21)

$V_{v1} = V_s + \dfrac{V_G}{2} \cdot \left[1 + \sin(\omega_G \cdot t)\right]$, volume *G* and line in *G* 1.f. (22)

$V_{v2} = V_s + \dfrac{V_G}{2} \cdot \left[1 - \sin(\omega_G \cdot t)\right]$, volume *G* and line in *G* 2.f. (23)

$V_s = V_G \cdot \alpha_s$ dead volume *G* (24)

Auxiliary hydraulic pump *PG*:

$Q_{tPG} = V_{pG} \cdot n_{sE} \cdot \eta_{QPG}$, theoretical flow *PG* (25)

$M_{PG} = \dfrac{V_{PG}}{2\pi} \cdot \dfrac{p_{t3}}{\eta_{mPG}}$ moment *PG* (26)

$Q_{zPG} = \dfrac{p_3}{R_{zPG}}$, flow leakage *PG* (27)

$Q_{cPG} = C_{PG} \cdot \dot{p}_3$, capacity flow *PG* (28)

$C_{PG} = \dfrac{V_{PG} + V_{vPG}}{K_K}$, line capacity *PG* (29)

Check valve flow *ZV1* 1.f. as shown in *Fig. 7*:

$$Q_{ZV1} = \frac{p_{G1} - p_3}{R_{ZV1}}, \quad \text{for } p_{G1} - p_3 \geq p_{mZV1}, \qquad (30)$$

$$Q_{ZV1} = 0, \qquad \text{for } p_{G1} - p_3 < p_{mZV1}. \qquad (31)$$

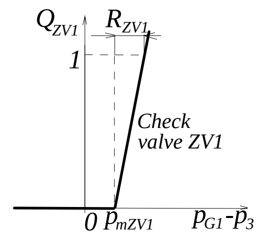

Fig. 7 Behavior of check valve flow ZV1

Check valve flow *ZV2* 2.f. as shown in Fig.8:

$$Q_{ZV2} = \frac{p_{G2} - p_3}{R_{ZV1}}, \quad \text{for } p_{G2} - p_3 \geq p_{mZV2}, \qquad (32)$$

$$Q_{ZV1} = 0, \qquad \text{for } p_{G1} - p_3 < p_{mZV1}. \qquad (33)$$

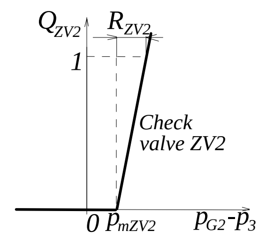

Fig. 8 Behavior of check valve flow ZV2

Check valve flow *ZV3 PG* as shown in Fig.9:

$$Q_{ZV3} = \frac{p_{t3} - p_3}{R_{ZV3}}, \quad \text{for } p_{t3} - p_3 \geq p_{mZV3}, \qquad (34)$$

$$Q_{ZV3} = 0, \qquad \text{for } p_{t3} - p_3 < p_{mZV3}, \qquad (35)$$

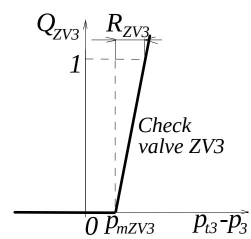

Fig. 9 Behavior of check valve flow ZV3

Hydraulic line *v*:

$p_{G1} - p_{v1} = R_{v1} \cdot Q_{G1}$,	pressure gradient in inner resistance R_{v1} 1.f.	(36)
$p_{v1} - p_{M1} = R_{v1} \cdot Q_{M1}$,	pressure gradient in inner resistance R_{v1} 1.f.	(37)
$Q_{M1} = Q_{G1} - Q_{cv1}$,	motor flow 1.f.	(38)
$p_{G2} - p_{v2} = R_{v2} \cdot Q_{G2}$,	pressure gradient in inner resistance R_{v2} 2.f.	(39)
$p_{M2} - p_{M2} = R_{v2} \cdot Q_{M2}$,	pressure gradient in inner resistance R_{v2} 2.f.	(40)
$Q_{M2} = Q_{G2} + Q_{cv2}$,	motor flow 1.f.	(41)
$Q_{cv1} = C_{v1} \cdot \dot{p}_{v1}$,	capacity flow 1.f.	(42)
$Q_{cv2} = C_{v2} \cdot \dot{p}_{v2}$,	capacity flow 2.f.	(43)

$C_{v1} = \dfrac{V_{v1}}{K_k}$, line capacity 1.f. (44)

$C_{v2} = \dfrac{V_{v2}}{K_k}$. line capacity 2.f. (45)

Hydraulic motor *M*:

$p_{M1} - p_{2M} = \dfrac{F_M}{S_M \cdot \eta_{mM}}$, pressure gradient in *M* (46)

$v_M = \dfrac{Q_{tM}}{S_M} \cdot \eta_{QM}$, velocity *M.* (47)

$h_M = \int v_M \cdot dt + h_{M0}$, piston-rod displacement *M.* (48)

$Q_{M1} = Q_{tM} + Q_{cM1} + Q_{zM1} - Q_{STV1} + Q_{HR1}$, flow *M* 1.f. (49)

$Q_{M2} = Q_{tM} - Q_{cM2} - Q_{zM2} + Q_{HR1} + Q_{STV2}$, flow *M* 2.f. (50)

$Q_{zM1} = \dfrac{p_{M1}}{R_{zM1}}$, flow leakage M 1.f. (51)

$Q_{cM1} = C_{M1} \cdot \dot{p}_{M1}$, capacity flow M 1.f. (52)

$C_{M1} = \dfrac{S_M \cdot \left(h_{mM}/2 + h_d + h_M\right) + V_{vM1}}{K_K}$, line capacity *M* 1.f. (53)

$Q_{zM2} = \dfrac{p_{M2}}{R_{zM2}}$, flow leakage *M* 2.f. (54)

$Q_{cM2} = C_{M2} \cdot \dot{p}_{M2}$, capacity flow *M* 2.f. (55)

$C_{M2} = \dfrac{S_M \cdot \left(h_{mM}/2 + h_d + h_M\right) + V_{vM2}}{K_K}$, line capacity *M* 2.f. (56)

Mechanical piston rod end position *M* as shown

$$F_d = k_d \cdot \left(h_M + \left(h_{mM} + h_d\right)\right), \text{ for } h_M < -\left(h_{mM} + h_d\right),$$

$$F_d = 0, \quad \text{for} - \left(h_{mM} + h_d\right) \le h_M \le \left(h_M + h_d\right),$$

$$F_d = k_d \cdot \left(h_M - \left(h_{mM} + h_d\right)\right), \text{ for } h_M > \left(h_{mM} + h_d\right), \qquad (57)$$

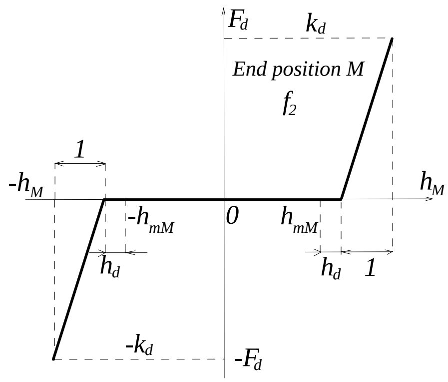

Fig. 10 Behavior of piston rod end position force of the motor M

Hydraulic distributor *HR2* (replacement of *HR2* and *SV* being considered as shown in *Fig. 1*):

$$Q_{HR2} = \frac{p_{M1} - p_{M2}}{R_{HR}} \cdot \varphi_{HR}, \qquad \text{for } 0 < \varphi_{HR} \le 1, \qquad (58)$$

$$Q_{HR2} = 0, \qquad \text{for } \varphi_{HR} = 0. \qquad (59)$$

Intake valve flow *DV PG* as shown in Fig.11:

$$Q_{DV} = \frac{p_{0DV} - p_3}{R_{DV}}, \qquad \text{for } p_3 \le p_{0DV} \text{ a } t>0, \qquad (60)$$

$$Q_{DV} = 0, \qquad \text{for } p_3 > p_{0DV}. \qquad (61)$$

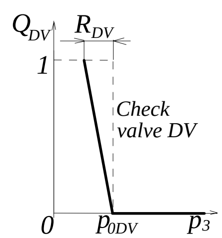

Fig. 11 Behavior of check valve flow ZV3

Stabilization valve flow *STV* of the motor *M* as shown on Fig.12:

$$Q_{STV1} = \frac{p_3 - p_{M1}}{R_{STV1}} \cdot f_{STV1}(h_M), \text{ for } p_3 \ge p_{M1}, \qquad (62)$$

$$Q_{STV1} = 0, \qquad \text{for } p_3 < p_{M1}, \qquad (63)$$

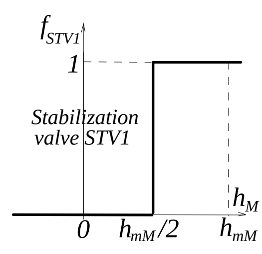

Fig. 12 Flow behavior of stabilization valve STV

Stabilization valve flow *STV* of the motor *M* as shown in *Fig. 13*:

$$Q_{STV2} = \frac{p_3 - p_{M2}}{R_{STV1}} \cdot f_{STV2}(h_M) \quad \text{for } p_3 \geq p_{M2}\,, \qquad (64)$$

$$Q_{STV2} = 0\,, \qquad \text{for } p_3 < p_{M2}\,, \qquad (65)$$

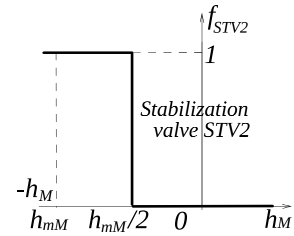

Fig. 13 Behavior of stabilization valve flow STV

Load (motor resistance *M* and load *Z* are merged):

, motion resistances M and Z. (66)

, mass of moving parts M and Z. (67)

$F_{M2} - F_{M3} = (F_{0M} + F_{0Z}) \cdot \mathrm{sgn}(v_M)$. solid friction forces M and Z (68)

Behavior of both pressures p_1, p_2 and pressure gradient Δp in phases is shown on *Fig. 14*. It is evident that starting phase of the mechanism is followed by stabilization of periodic course.

Behavior of the same pressures while increasing the load weight to m = 8 kg is shown in *Fig. 15*. Pressures get stabilized later which results from deformation of a liquid column in phases, flow leakage in phases and the necessary replenishment of single phases. Pressure gradient amplitude Δp is higher.

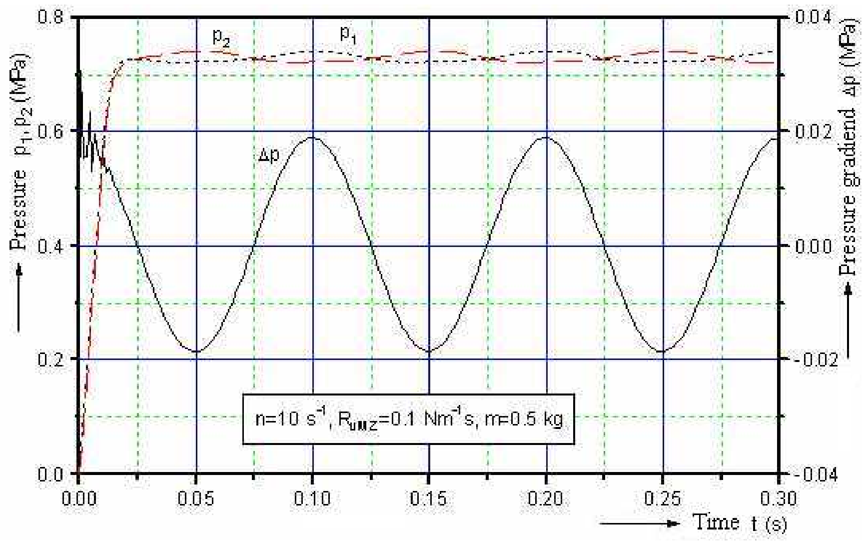

Fig. 14 Behavior of pressures p_1, p_2, Δp in phases at $n = 10\ s^{-1}$, $R_{vMZ} = 0.1\ N{\cdot}m^{-1}{\cdot}s$, $m = 0.5$ kg

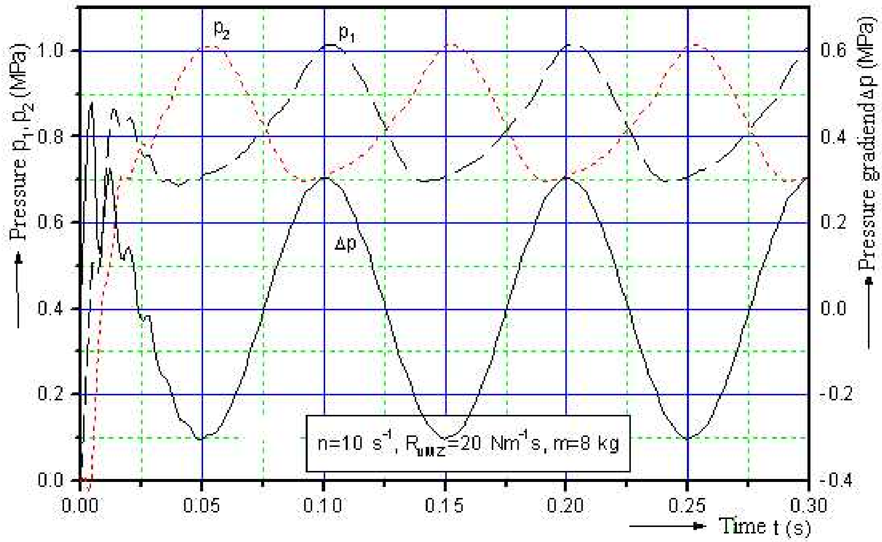

Fig. 15 Behavior of pressures p_1, p_2, Δp in phases at n = 10 s^{-1}, R_{vMZ}= 0.1 $N{\cdot}m^{-1}{\cdot}s$, m = 8 kg

In *Fig. 16*, we used the same parameters as in *Fig. 14*, however the hydraulic pump rational speed was increased to n = 25 s^{-1}. As a consequence, the period for pressure stabilization got longer, overshoots in the start phase as well as the degree of their shape deformations following the stabilization process were increased.

Following the pressure behavior, we can say that in the case shown in *Fig. 16*, the pressure of the pressure valve *TV3* (p_3) would have to be increased so that the pressure would not have dropped below a pressure value of saturated steams of the fluid used.

Fig. 17 illustrates increased rational speed of the hydraulic pump to n = 25 s^{-1}, increased viscous damping coefficient to R_{vMZ} = 20 $N{\cdot}m^{-1}{\cdot}s$ and the load mass to m = 8 kg. As a result, the period of pressure stabilization, overshoots in the start phase became longer, and the degree of their deformation was substantially higher after the process stabilization. The highest increase was observed in the overshoot of the pressure p_1 to negative values that must not occur in real operations. Following the pressure behavior, we can conclude that as shown in *Fig. 16*, the pressure of the pressure control valve *TV3* (p_3) would have to be increased in order not to have dropped below the pressure value of the saturated steams of the fluid used.

Figure *Fig. 18* shows the behavior of pressure gradients Δp and Δp at both constant and variable loads applying the force F_{M3} that does not depend on hydraulic motor speed in the range of +100 N up to -100 N in the time period of 0.3 sec to 0.7 sec. The behavior illustrates the hydraulic pump rational speed n = 10 s^{-1}, viscous friction coefficient of R_{vMZ} = 20 $Nm^{-1}s$ and the mass of both hydraulic motor and load m = 8 kg.

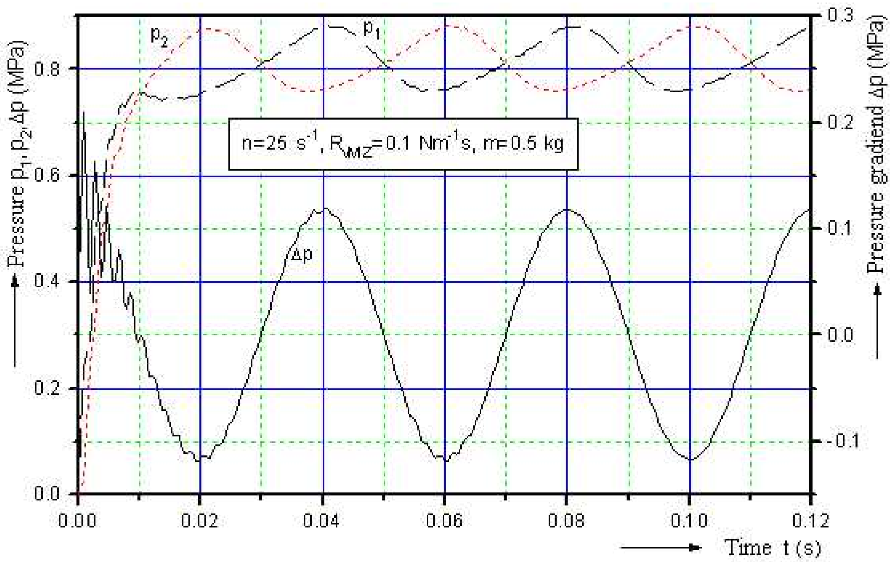

Fig. 16 Behavior of pressures p_1, p_2, Δp in phases at $n = 25\ s^{-1}$, $R_{vMZ} = 0.1\ N{\cdot}m^{-1}{\cdot}s$, $m = 0.5$ kg

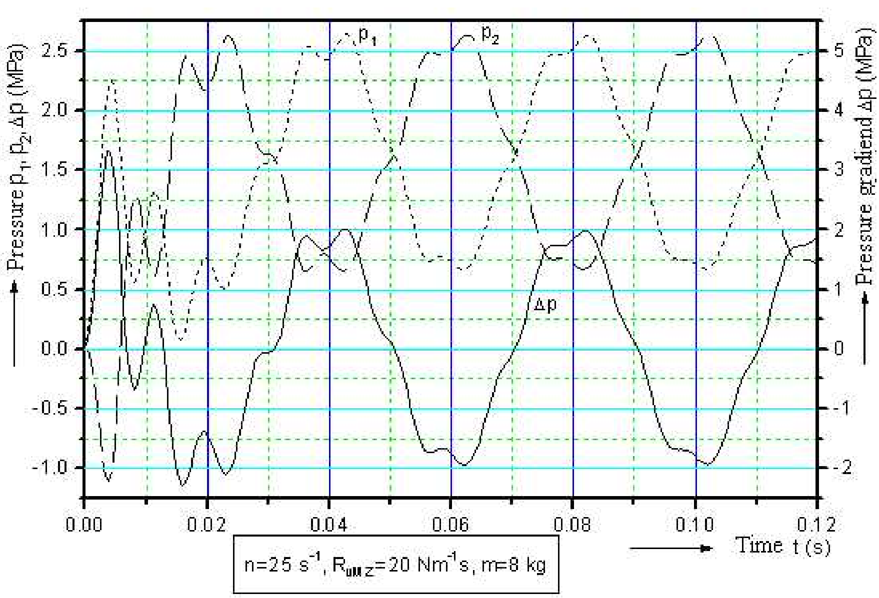

Fig. 17 Behavior of pressures p_1, p_2, Δp in phases at $n = 25\ s^{-1}$, $R_{vMZ} = 20\ N{\cdot}m^{-1}{\cdot}s$, $m = 8$ kg

When applying the variable force F_{M3} there is a ripple in the pressure gradient Δp_1 coming from transmission frequencies themselves. For confronting purposes, we provide a course of pressure gradient Δp without applying the variable load F_{M3}. Once the variable load is not applied, the pressure gradient course is attenuated in a short time.

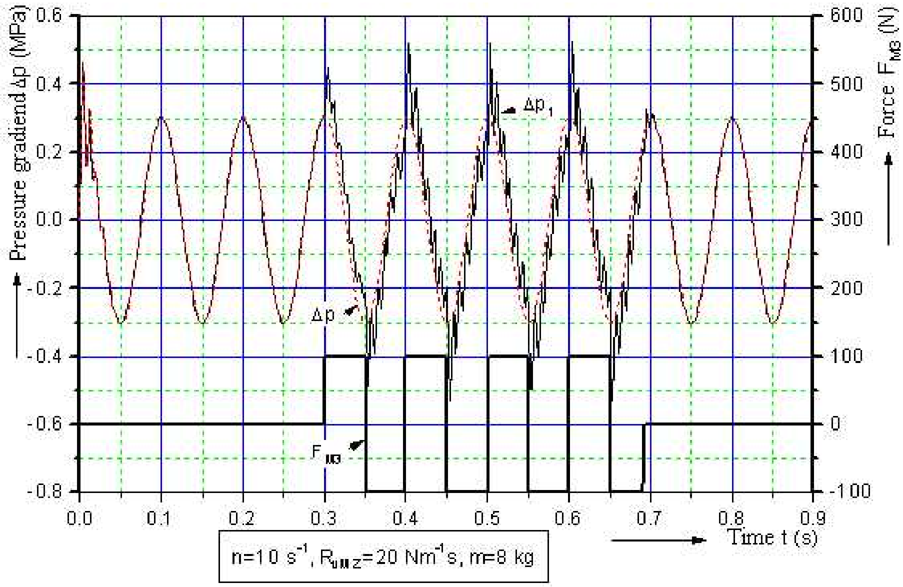

Fig. 18 Pressure gradient behavior Δp, Δp_1 with harmonized variable load F_{M3}

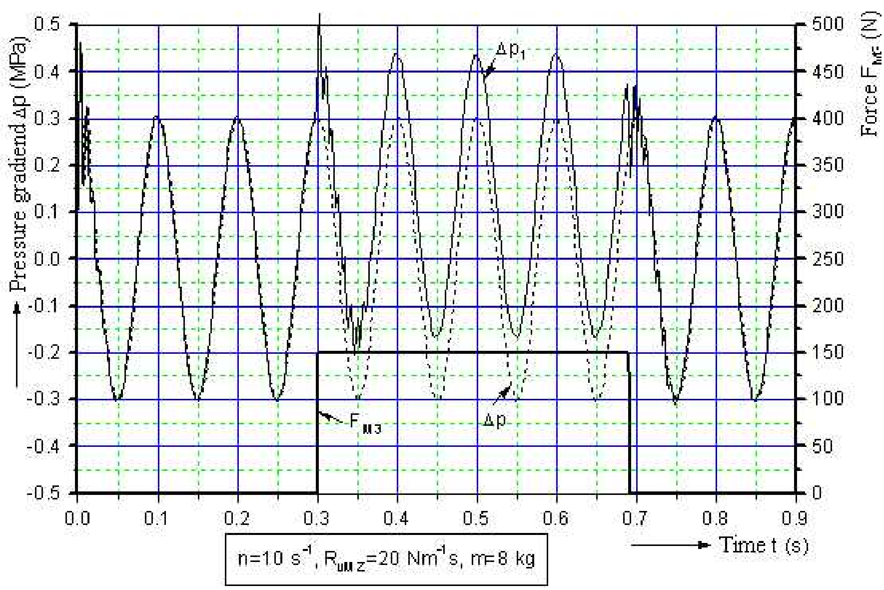

Fig. 19 Behavior of pressure gradients Δp, Δp_1 with single-side variable load F_M

Figure *Fig. 20* illustrates the behavior of hydraulic motor h_M and h_{M1} strokes under the same conditions as aforementioned. The course of h_M stroke (solid line) shows no application of the force F_{M3} and the course of h_{M1} stroke (dotted line) shows single-side application of the load coming from the force F_{M3}. Due to the effect of this single-side load given by the forceF_{M3}, the central position of the stroke is shifted in the same direction as the action of this force, thus it is necessary to fit the mechanism with a built-in central position stabilizer – as proposed in *Fig. 1*.

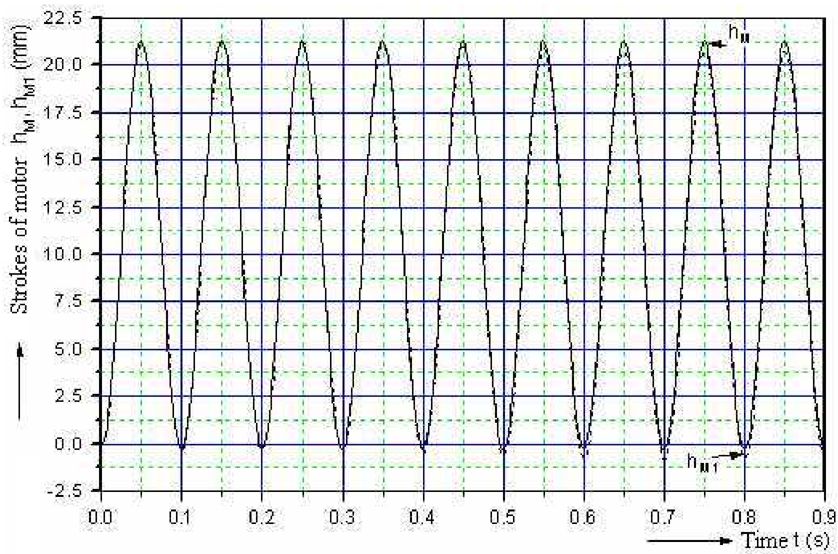

Fig. 20 Behavior of piston rod strokes of the hydraulic motor h_M and h_{M1} with single-side variable load F_{M3}

We made the analysis by means of the DYNAST software. Was she would appropriate do analyse too with ecological fluid.

4. CONCLUSIONS

We made a dynamic analysis of the mechanism by means of methods used in mechatronic systems (as shown in e.g. [1, 2, 3, 4, 5, 7]). Thus, we were able to analyze the dynamic behavior of both inner and external mechanical and hydraulic values of a two-phase hydraulic motor with the fluid alternating flow. Based on the analysis results, we can draw conclusions that despite of the fact that the double – phase mechanism with fluid alternating flow has stabilizing effects for maintaining the central position, it is necessary to use an additional mechanism to stabilize the central position of the hydraulic motor when applying heavy single-side loads. While designing such mechanisms, it is a must to analyze the hydraulic circuit values thoroughly to prevent them from being incorrect. It is necessary e.g. to keep the circuit pressure from dropping below the saturated steams pressure value of the hydraulic power carrier. This issue also requires having appropriate dynamic properties of pressure control and check valves in place to replenish any fluid leakages in a quick and efficient manner.

The paper was developed under VEGA MŠ SR grant „The research of making more effective ecological aspect operation of mobile and stationary technique in agriculture". No. 1/3483/06.

Lektoroval: Prof. Ing. Josef Koreis, CSc.

Předloženo: 27.3.2006.

References

1. KOREISOVÁ Gabriela: *Reliability ensuring using parametric similarity in design*. In: Int. Conf. Reliability and Diagnostics of Transport Structures and Means 2005, pp. 158 -166, (2005). ISBN 80-7194-769-5.
2. KRCHNÁR Jozef, STRAČÁR Karol: *Možnosti diagnostikovania technického stavu hydraulických systémov*. In: HYDRAULIKA A PNEUMATIKA. Časopis pre hydrauliku, pneumatiku a automatizačnú techniku. Ročník 2, 1/2000. ISSN 1335-5171. s.18÷20.
3. NEVRLÝ Josef: *Methodology of modelling fluid power and lubrification systems. Selected aspects*. WYDAW. POLITECHNIKI WROCLAWSKEJ, Wroclaw 2005. ISBN 83-7085-848-1.
4. PAVLOK B.: *Dynamické vlastnosti hydraulického pohonu řízeného proporcionálním rozváděčem*. In: Medzinárodná vedecká konferencia HYDRAULIKA A PNEUMATIKA 2004. Svit, 29.9.-1.10.2004. s. 145 - 148. ISBN 80-968961-2-1.
5. PRIKKEL Karol: *Riešenie pohybu piesta hydromotora v prostredí Matlab-u*. In: HYDRAULIKA A PNEUMATIKA, IV, 2002, č.1 (8).. s.37-38. ISSN 1335-5171.
6. TKÁČ Zdenko, DRABANT Štefan, JABLONICKÝ J., KLEINEDLER Peter: *Skúšky hydrostatického motora s ekologickou kvapalinou*. In.: Acta technologica agriculturae, roč. 7, 2004, č. 1, s. 14-19. ISSN 1335-2555.
7. TURZA Jozef, PETRANSKÝ Ivan, JURČO Ivan, TKÁČ Zdenko: *Dvojfázové hydraulické mechanizmy so striedavým prietokom kvapaliny*. Vedecká monografia. Trenčín: Vydala Trenčianska univerzita AD v Trenčíne 2005. 242s. ISBN 80-8075-071-8.

Resumé

DYNAMIKA DVOJFÁZOVÉHO MECHANIZMU SPK S PRIAMOČIARYM HYDROMOTOROM

Josef TURZA, Monika GULLEROVÁ

U klasických hydraulických mechanizmov je prietok kvapaliny vo vedení medzi hydrogenerátorom a hydromotorom jednosmerný. V mechanizmoch so striedavým prietokom kvapalina vo vedení vykonáva vratný pohyb. Tlak a prietok má v ustálenom stave periodický priebeh. Mechanizmov so striedavým prietokom kvapaliny, (ďalej len SPK), je z hľadiska počtu fáz viacej druhov. Najväčšie uplatnenie nachádzajú dvojfázové mechanizmy so SPK. Sú vhodné všade tam, kde je potrebný trvalý striedavý pohyb výkonného člena, ako sú napr. poľnohospodárske kosačky,

vytriasacie mechnismy strojov, textilné tkacie stavy, zariadenia pre únavové skúšky a pod. Oproti klasickým vačkovým, alebo kľukovým mechanizmom majú výhodu nezávislého priestorového usporiadania na strojnom zariadení a jednoduchú možnosť ochrany voči preťaženiu. Pre posúdenie funkčných vlastnosti dvojfázového mechanizmu je dôležitá jeho dynamická analýza, urobená v predloženom príspevku.